Chaos, Solitons & Fractals 44 (2011) 982–989

Contents lists available at SciVerse ScienceDirect

Chaos, Solitons & Fractals

Nonlinear Science, and Nonequilibrium and Complex Phenomena

journal homepage: www.elsevier.com/locate/chaos

Replicate periodic windows in the parameter space of driven oscillators

E.S. Medeiros [a,*], S.L.T. de Souza [b], R.O. Medrano-T [c], I.L. Caldas [a]

[a] Instituto de Física, Universidade de São Paulo, São Paulo, Brazil
[b] Universidade Federal de São João del-Rei, Campus Alto Paraopeba, Minas Gerais, Brazil
[c] Departamento de Ciências Exatas e da Terra, Universidade Federal de São Paulo, Diadema, São Paulo, Brazil

ARTICLE INFO

Article history:
Received 12 May 2011
Accepted 17 August 2011
Available online 9 September 2011

ABSTRACT

In the bi-dimensional parameter space of driven oscillators, shrimp-shaped periodic windows are immersed in chaotic regions. For two of these oscillators, namely, Duffing and Josephson junction, we show that a weak harmonic perturbation replicates these periodic windows giving rise to parameter regions correspondent to periodic orbits. The new windows are composed of parameters whose periodic orbits have the same periodicity and pattern of stable and unstable periodic orbits already existent for the unperturbed oscillator. Moreover, these unstable periodic orbits are embedded in chaotic attractors in phase space regions where the new stable orbits are identified. Thus, the observed periodic window replication is an effective oscillator control process, once chaotic orbits are replaced by regular ones.

1. Introduction

The parameters of deterministic dynamical systems play an important role in specifying the transitions between chaotic and periodic behavior. This parameter influence on the attractor transition can be represented in the parameter space [1–5]. In particular, for both discrete-time [1,6] and continuous dynamical systems [7], it is known that the set of parameters for which a system exhibits periodic behavior are periodic windows immersed in chaotic regions, in the form of shrimps, in the bi-dimensional parameter space. In the past two decades, periodic windows have been numerically obtained for a large number of applied dynamical systems like lasers [8,9], electronic circuits [9–11], mechanical oscillators [12], and also in population dynamics [13]. Periodic windows have also been identified in experiments with electronic circuits [14–16].

Additionally, the bi-dimensional parameter diagram is an important tool to analyze the control of chaos, by introducing periodic perturbations, allowing a global overview of periodic and chaotic behavior [17]. However, despite several articles reporting this kind of control, it still remained to be determined how the parameter space changes with the control.

Suppression of chaos by adding a weak harmonic perturbation has been numerically and theoretically reported specially for systems with an original harmonic driven [18–20]. For example, a weak harmonic perturbation has been used to suppress chaos in the forced Duffing oscillator [21], and a similar perturbation has been applied to control chaos in a Josephson junction oscillator [22]. Considering that in [21,22] the controlling of these two well known systems were essentially accomplished for limited ranges of system parameters, a further parameter space analysis considering a weak harmonic perturbation is required. Moreover, it still remained to be determined how the controlled orbit parameters were distributed in the parameter space.

A weak harmonic forcing, applied to an impact-pair system, generates, in the bi-dimensional parameter space, new periodic windows near the unperturbed one with its shape and periodicity [17]. The new periodic windows are parameter sets for which the controlled periodic orbits substitute the chaotic orbits. However, as the parameter space alteration was reported for non smooth systems described by discrete time dynamics, further investigation

* Corresponding author. Tel.: +55 (11) 3091 6842; fax: +55 (11) 3091 6706.
E-mail address: esm@if.usp.br (E.S. Medeiros).

0960-0779/$ - see front matter © 2011 Elsevier Ltd. All rights reserved.
doi:10.1016/j.chaos.2011.08.002

should verify the parameter space alteration that would be produced by harmonic perturbations in continuous time systems.

The main motivation of this article is to determine the alterations in the parameter space due to weak harmonic perturbations applied to smooth continuous time dynamical systems. To investigate that, we analyze how such perturbations modify the attractors and the parameter space of the harmonically driven Duffing and Josephson oscillators. We find that the additional harmonic perturbations considered in this work control some chaotic orbits that become periodic and whose parameters form new periodic windows in the parameter space embedded in the remaining chaotic region. For the first time in the literature, we observe that this harmonic perturbation replicates the periodic windows in the parameter space of these systems. Moreover, we find evidences that new periodic orbits, whose parameters are in the new periodic windows, have the same periodicity and pattern of both stable periodic orbits already existing and unstable periodic orbits embedded in the unperturbed chaotic attractor. Additionally, these unstable periodic orbits are embedded in chaotic attractors in the phase space region where the new stable orbits are identified. Thus, the observed periodic window replication is an effective oscillator control process, once chaotic orbits are replaced by regular ones.

This article is organized as follows: in Section 2, we obtain the parameter space of the unperturbed Duffing oscillator and we establish the suitable parameters to implement the weak perturbation. In Section 3, for the Duffing oscillator, we investigate the periodicity, shape and Lyapunov exponents of the perturbed periodic and of the unperturbed chaotic orbit. In Section 4, we present, for the Josephson oscillator, another example of replicate periodic windows caused by a weak periodic perturbation. Finally, in Section 5 we summarize our main conclusions.

2. Parameter space structure of the Duffing oscillator

The Duffing oscillator is a well-known model to describe oscillations of a mass obeying a fourth order symmetric potential [23]. This system has a large number of applications, specially to model physical systems, and has been extensively studied in theoretical, numerical and experimental approaches [24–26]. Here, we consider a simple version of the Duffing system, which describes oscillations of a single-well potential.

The time evolution of this system is determined by solution of the following dimensionless equation:

$$\frac{d^2x}{dt^2} + c\frac{dx}{dt} + x^3 = \beta\cos(\omega t). \tag{1}$$

Here, the parameter c is the amplitude of the system damping, β is the forcing amplitude, and ω is the driven frequency settled at $\omega = 1.0$. We numerically obtain solutions of the Duffing equation by using a fourth-order Runge–Kutta method with fixed step $h = 0.001$.

Additionally, to investigate transitions between chaotic and periodic attractors of the Duffing oscillator, the largest non zero Lyapunov exponent is obtained [27] for each point of a bi-dimensional grid of the system parameters (parameter space).

In Fig. 1, we show the bi-dimensional parameter space $(c \times \beta)$ obtained for the Duffing oscillator (also shown in [25]). The Lyapunov exponent features of each point in the grid are represented by assigning different colors. In Fig. 1, blue color represents parameter sets for which the attractors are chaotic (positive Lyapunov exponent), while grey-scale represents parameter sets for which the attractors are periodic (negative Lyapunov exponent). In black we represent points close to the superstable lines corresponding to periodic attractors for which the largest non zero Lyapunov exponents is a minimum inside a periodic window.

We observe, in Fig. 1, that the parameter sets for which the Duffing oscillator behaves periodically are in aggregated periodic windows (gray scale area). Those periodical structures, also known as shrimps, have been well described in literature [1–3]. In Fig. 1(b), the red point and the black plus symbol indicate examples of parameter sets whose orbits are, respectively, periodic and chaotic; these two orbits will be further considered in Section 3.

To show the different behavior of the two attractors associated with the two parameter sets marked in Fig. 1(b), we obtain a stroboscopic map by collecting the velocity and the displacement at time t multiple of $2\pi/\omega$, where ω is the driven frequency. In Fig. 2(a), we show the periodic orbit with parameters indicated by the red[1] point symbol inside the periodic window amplified in Fig. 1(b). Likewise, in Fig. 2(b) we show the chaotic attractor for parameters represented by a black plus symbol in Fig. 1(b).

We call the attention that the periodic and chaotic attractors, shown in Fig. 2, although obtained for different parameters are in the same phase space region. Next, in Section 3, we analyze how these two orbits are modified by a weak periodic perturbation.

3. Introducing a weak perturbation in the Duffing oscillator

We introduce a weak harmonic perturbation by adding a second harmonic term in the original Duffing driven. The perturbation amplitude is taken as a control parameter of the system. On the other hand, the perturbation frequency is settled in an integer ratio of the original system frequency. Similar procedures have been already reported in literature [19–22]. So, the time evolution of this perturbed system is determined by the solution of the following dimensionless equation:

$$\frac{d^2x}{dt^2} + c\frac{dx}{dt} + x^3 = \beta\cos(\omega t) + \alpha\sin(\Omega t). \tag{2}$$

Here, α is the weak perturbation amplitude ($\alpha \ll \beta$) and Ω is the perturbation frequency fixed at $\Omega = 2\omega$. Other rational multiples of ω could be used to Ω [17,21].

In Fig. 3, we present the parameter space of the perturbed Duffing oscillator for two different perturbation

[1] For interpretation of color in Figs. 2, 3 and 8, the reader is referred to the web version of this article.

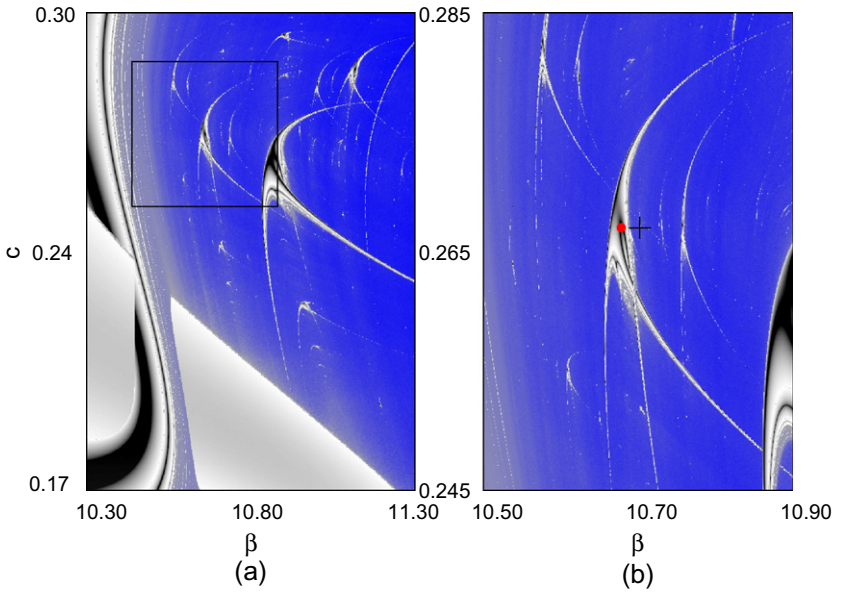

Fig. 1. (a) Bi-dimensional ($c \times \beta$) parameter space of the unperturbed Duffing oscillator, for $\omega = 1.0$. (b) Magnification of the squared area. The red circle indicates periodic behavior at $\beta = 10.6780$ and $c = 0.2670$, the black plus symbol indicates chaotic behavior at $\beta = 10.7020$ and $c = 0.2670$. (For interpretation of the references to colour in this figure legend, the reader is referred to the web version of this article.)

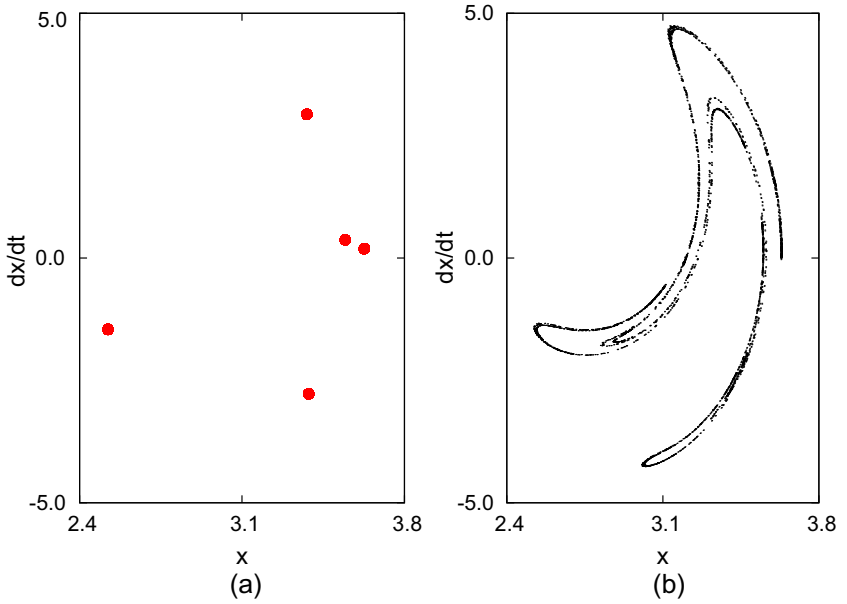

Fig. 2. Stroboscopic phase space of the Duffing oscillator. (a) Periodic orbit correspondent to the parameters $\beta = 10.6780$ and $c = 0.2670$ (red circle in Fig. 1(b)). (b) Chaotic attractor correspondent to the parameters $\beta = 10.7020$ and $c = 0.2670$ (black plus symbol in Fig. 1(b)).

amplitudes $\alpha = 0.04$ and $\alpha = 0.08$. By comparing the parameter spaces of Fig. 1(b) and Fig. 3(a) and (b), we note the existence of replicated periodic windows. In particular, the central periodic window of Fig. 1(b) is duplicated in Fig. 3.

Moreover, the periodic windows appear slightly displaced in Fig. 3(a) and (b). In Fig. 3 we mark a red point and a black plus symbol to indicate the parameters of the periodic and chaotic orbits shown in Fig. 1(a). Note that in Fig. 3(a), for the perturbation amplitude $\alpha = 0.04$, the black plus still represents a chaotic orbit, while in Fig. 3(b), for the perturbation amplitude $\alpha = 0.08$, the black plus represents a periodic orbit inside a replicated periodic window. On the other hand, the former periodic orbit with parameters represented by the red point is still periodic in Fig. 3(a) and chaotic in Fig. 3(b). Thus, the periodic perturbation, which changes the attractors, modifies the parameter space generating periodic window replications

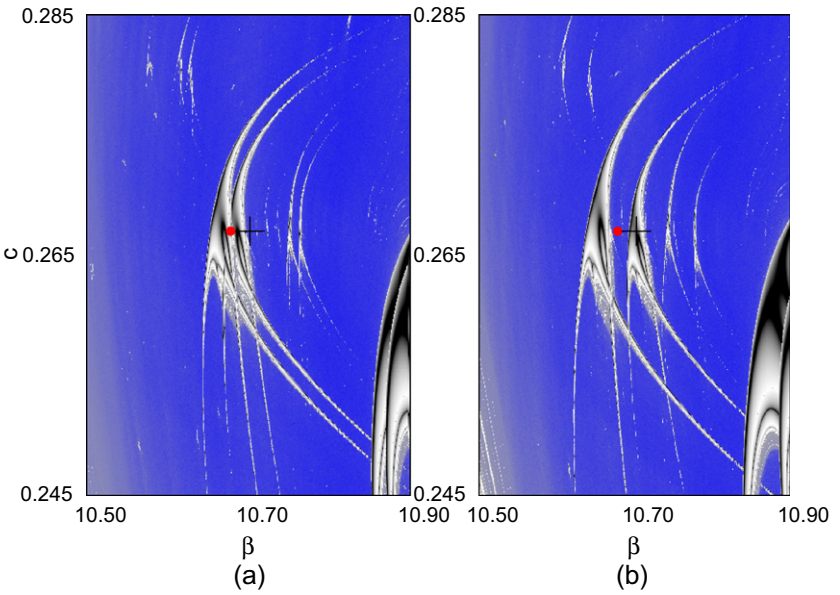

Fig. 3. Bi-dimensional ($c \times \beta$) parameter space of the perturbed Duffing oscillator for $\omega = 1.0$ and $\Omega = 2.0$. The perturbation amplitude is $\alpha = 0.04$ in (a) and $\alpha = 0.08$ in (b).

separated by a distance that increases with the perturbation amplitude. We emphasizes that the former chaotic attractor, shown in Fig. 2(a), has been changed to a periodic one, one example of control of chaos by a periodic perturbation.

Next, we discuss the alteration that the weak perturbation produces on the chaotic orbit shown in Fig. 2(b). For this purpose, in Fig. 4(a) we show the stroboscopic phase space of the controlled periodic orbit (in black plus symbols) that substitutes the former chaotic orbit shown in Fig. 2(b). Besides, this controlled orbit has the same periodicity and pattern of the unperturbed periodic orbit shown in Fig. 2(a) and reproduced in Fig. 4(a) (in red points). Moreover, in Fig. 4(b) we show the time convergence of the largest non zero Lyapunov exponent of the two orbits of Fig. 4(a). These orbits have similar Lyapunov exponent convergence reaching comparable limit values.

The described orbit resemblances present in Fig. 4 could be an indication that the controlled periodic orbit already exists as an unstable periodic orbit in the unperturbed system. To verify this possibility, we next investigate the relation between the controlled periodic orbit and a possible unstable periodic orbit embedded in the chaotic attractor. Thus, to find an approximation of the unstable orbit, we integrate the unperturbed equation for a short integration time and parameters indicated by the black plus symbol in Fig. 1(b), corresponding to a chaotic attractor. This procedure can reveal the unstable orbit embedded in such attractor. Moreover, to facilitate the identification of the desired unstable periodic orbit, for the integration we choose initial conditions in the controlled orbit indicated by black plus symbols in Fig. 4(a).

Accordingly, in Fig. 5, for the orbits discussed in the previous paragraph, we show the stroboscopic map composed by the velocity, dx/dt, and the displacement, x, at time t multiple of $2\pi/\omega$ (where ω is the driven frequency). In this figure, the blue triangle symbol denotes the unstable orbit found during the described short integration time. In this interval such unstable orbit has the same periodicity and pattern of the mentioned unperturbed periodic orbit (in red points) and the controlled periodic orbit (black plus symbol).

The analysis of results shown in Figs. 4 and 5 indicates that the generated new periodic windows are composed of parameters for which periodic orbits are in a phase space region where unstable periodic orbits were embedded in a chaotic attractor.

4. Weak periodic perturbation in the Josephson junction oscillator

The superconducting Josephson junction is usually modeled by an electronic circuit equation [28]. Considerable efforts has been devoted to understand the onset of chaos in this system and its critical parameters for this transition [29–31]. The system is described by a pendulum-like dimensionless equation [22]:

$$\frac{d^2\phi}{dt^2} + G\frac{d\phi}{dt} + \sin\phi = I + A\sin(\omega t). \tag{3}$$

Here, the parameter G gives the amplitude of the system damping, I is the direct current component of the circuit, ω is the driven frequency settled at $\omega = 0.25$, while A is the alternating current component of the circuit and the system forcing amplitude.

In Fig. 6, we obtain the bi-dimensional parameter space ($G \times A$) of the Josephson oscillator given by Eq. (3). In this figure, blue points correspond to positive Lyapunov exponent (chaotic behavior), while grey- scale points correspond to negative Lyapunov exponent (periodic behavior). The black region corresponds to the superstable lines.

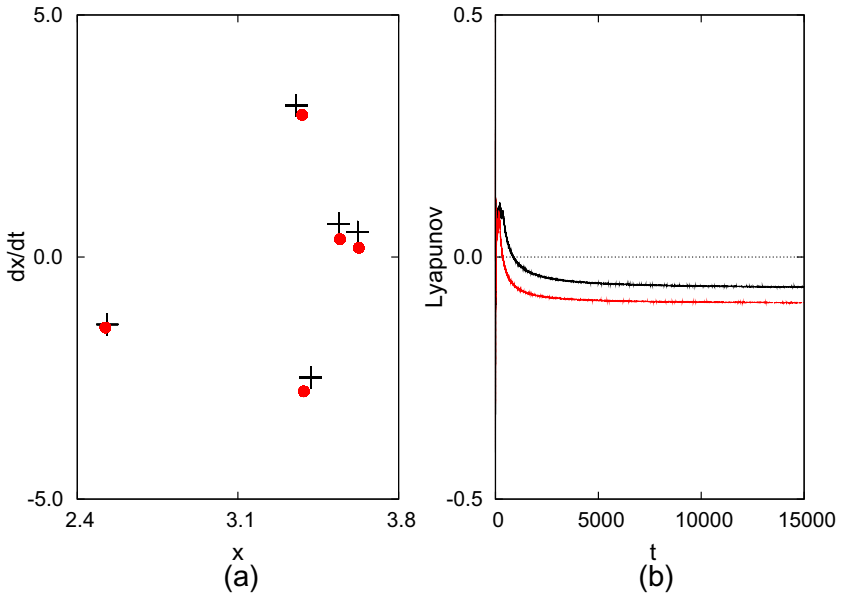

Fig. 4. (a) The red circle symbol denotes the periodic orbit for $\beta = 10.6780$, $c = 0.2670$ and $\alpha = 0.0$, the same orbit of Fig. 2(a). The black plus symbol denotes the controlled orbit for $\beta = 10.7020$, $c = 0.2670$, $\Omega = 2.0$, and $\alpha = 0.08$. (b) The red line indicates the largest Lyapunov exponent of the unperturbed periodic orbit. The black line indicates the largest Lyapunov exponent of the controlled orbit. (For interpretation of the references to colour in this figure legend, the reader is referred to the web version of this article.)

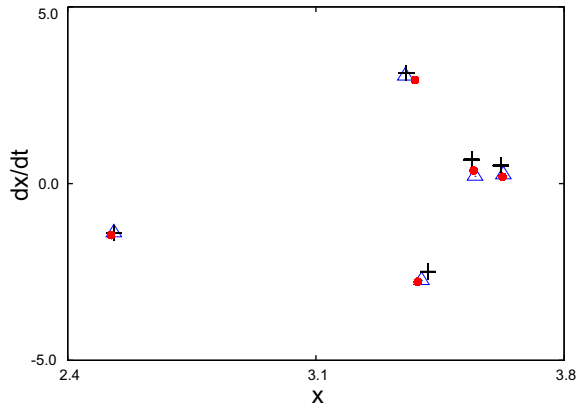

Fig. 5. The blue triangle indicates the chaotic orbit under a short integration time for $\beta = 10.7020$, $c = 0.2670$ and $\alpha = 0.0$. The black plus symbol indicates the controlled periodic orbit for $\beta = 10.7020$, $c = 0.2670$, $\alpha = 0.08$ and $\Omega = 2.0$. The red circle symbol indicates the unperturbed periodic orbit for $\beta = 10.6780$, $c = 0.2670$ and $\alpha = 0.0$. (For interpretation of the references to colour in this figure legend, the reader is referred to the web version of this article.)

We verify, in Fig. 6, the existence of aggregated periodic windows in the parameter space of the Josephson oscillator. As in Fig. 1(b), the red point and the black plus symbol indicate in Fig. 6(b) examples of parameters for which the correspondent orbits are, respectively, periodic and chaotic.

For the two attractors associated with the parameter sets marked in Fig. 6(b), we present in Fig. 7(a) and (b) the stroboscopic map obtained by collecting the variable $\phi \pmod{2\pi}$ and its time derivative, $d\phi/dt$, at time t multiple of $2\pi/\omega$. Thus, Fig. 7(a) and (b) show, respectively, the mentioned periodic and chaotic attractors to be further analyzed in this section. The periodic and chaotic attractors, shown in Fig. 7, although obtained for different parameters are in the same phase space region. Next, we analyze how these two orbits are modified by a weak periodic perturbation.

For the Josephson oscillator, similarly to the perturbed Duffing oscillator (considered in Section 3), a harmonic term is added to the original one:

$$\frac{d^2\phi}{dt^2} + G\frac{d\phi}{dt} + \sin\phi = I + A\sin(\omega t) + \alpha\sin(\Omega t), \tag{4}$$

where, α is the perturbation amplitude and Ω is the perturbation frequency fixed at $\Omega = \omega/2$.

In Fig. 8 we present the parameter space of the perturbed Josephson oscillator for two different perturbation amplitudes $\alpha = 0.005$ and $\alpha = 0.01$. In this case, similarly to what was noticed in Fig. 3 for the Duffing oscillator, the existence of replicate periodic windows in the modified parameter space is also observed. In Fig. 8 we mark a red point and a black plus symbol to indicate the parameters of the periodic and chaotic orbits shown in Fig. 6(b). Note that in this figure the black plus represents a controlled periodic orbit inside a replicated periodic window, while the orbit with parameters represented by the red point continues periodic in Fig. 8. Moreover, comparing Fig. 8(a) and (b), we also observe that the periodic window displacement slightly increases with the perturbation amplitude, as observed in Fig. 3 for the Duffing oscillator parameter space. Thus, the periodic perturbation, which changes the attractors, modifies the parameter space generating periodic window replications separated by a distance that increases with the perturbation amplitude. The changing of the chaotic attractor, shown in Fig. 7(b), to a periodic one, can

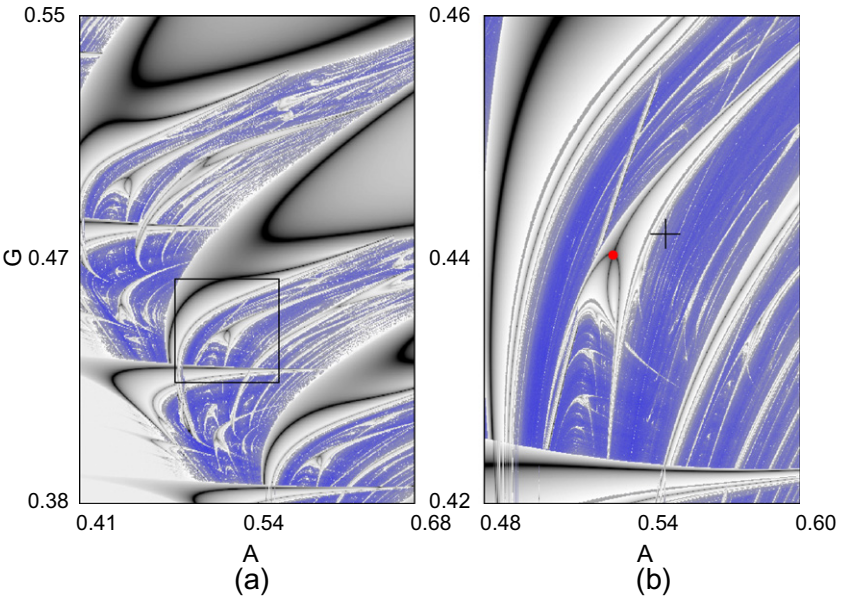

Fig. 6. (a) Bi-dimensional ($G \times A$) parameter space of the unperturbed Josephson oscillator, the natural system frequency is settled for $\omega = 0.25$, the direct current component is settled for $I = 0.905$. (b) Magnification of the squared area. The red circle indicates the parameters $A = 0.5289$ and $G = 0.4403$, the black plus symbol indicates the parameters $A = 0.5488$ and $G = 0.4416$. (For interpretation of the references to colour in this figure legend, the reader is referred to the web version of this article.)

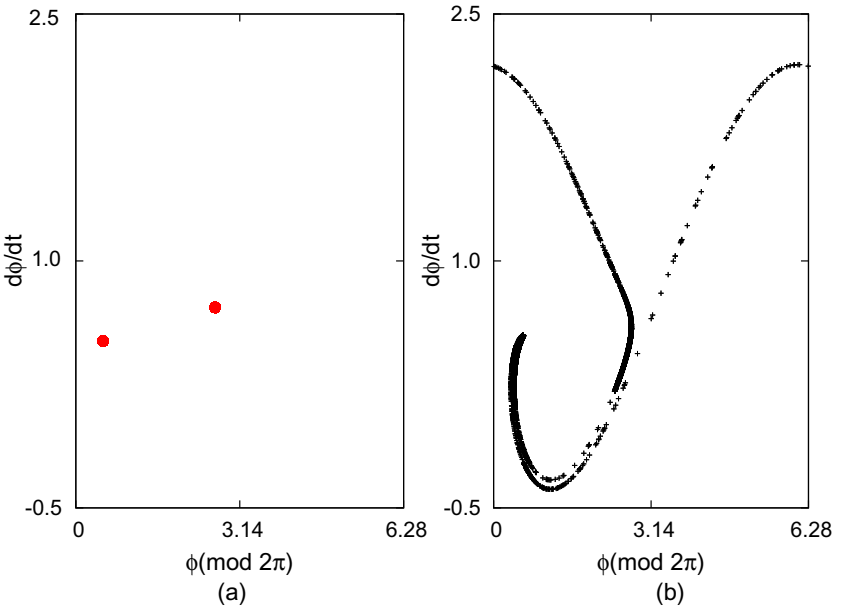

Fig. 7. Stroboscopic phase space of Josephson oscillator. (a) Periodic orbit correspondent to the parameters $A = 0.5488$ and $G = 0.4416$ (red circle in Fig. 6(b)). (b) Chaotic attractor correspondent to the parameters $A = 0.5488$ and $G = 0.4416$ (black plus symbol in Fig. 6(b)). (For interpretation of the references to colour in this figure legend, the reader is referred to the web version of this article.)

be considered one example of control of chaos by a periodic perturbation.

Next, to show how these orbits are modified by the considered perturbation with amplitude $\alpha = 0.01$, we present in Fig. 9 the stroboscopic mapping (with sampling period proportional to the driven frequency inverse) of the periodic orbit indicated in Fig. 7(a) (indicated by red points), the controlled periodic orbit (indicated by black plus symbols), and an identified unstable orbit embedded in the chaotic attractor of Fig. 7(b) (blue triangles). To identify the unstable orbit we followed the procedure indicated in Section 3.

Thus, the results shown in Figs. 6–9 confirm the evidence, find for the Duffing oscillator, that periodic window

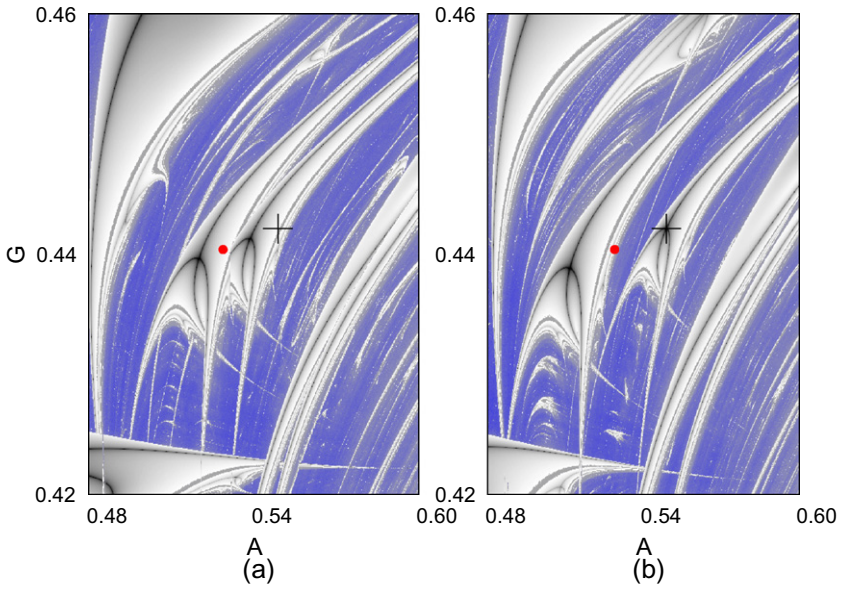

Fig. 8. Bi-dimensional ($G \times A$) parameter space of the perturbed Josephson oscillator, the natural system frequency and the perturbation frequency are settled, respectively, for $\omega = 0.25$ and $\Omega = 0.125$. (a) The perturbation amplitude is settled for $\alpha = 0.005$. (b) The perturbation amplitude is settled for $\alpha = 0.01$.

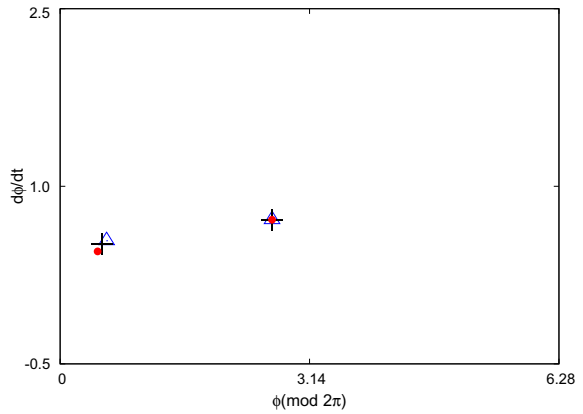

Fig. 9. The blue triangle indicates the chaotic orbit under a short integration time for $A = 0.5488$, $G = 0.4416$ and $\omega = 0.25$. The black plus symbol indicates the controlled periodic orbit for $A = 0.5488$, $G = 0.4416$, $\omega = 0.25$ and $\Omega = 0.125$. The red circle symbol indicates the previous periodic orbit for $A = 0.5488$, $G = 0.4416$ and $\omega = 0.25$. (For interpretation of the references to colour in this figure legend, the reader is referred to the web version of this article.)

replications in parameter space correspond to periodic orbit onset in phase space regions where unstable periodic orbits were embedded in chaotic attractors.

5. Conclusions

We investigate the periodic orbit onset for two driven oscillators due to a weak harmonic forcing. To identify periodic and chaotic regions in the bi-dimensional parameter space, we compute the largest non zero Lyapunov exponents for the attractors in the considered parameter ranges. We identify shrimp shaped periodic windows immersed into a chaotic region. The parameter space is much modified whenever a weak amplitude forcing is applied. We perform local analysis of the parameter space and find regions where new periodic windows arising in the neighborhood of the original windows. However, a global analysis of the parameter space reveals other kind of alterations as the periodic window destruction or no window replication.

By analyzing stroboscopic maps of unperturbed and perturbed attractors we find evidences that the new reported periodic windows are formed by parameters for which the observed new periodic attractors have the same periodicity and pattern as those preexisting stable and unstable periodic orbits. Therefore, we find that the replicate periodic windows reported in this work are due to periodic orbit onset in phase space regions where unstable periodic orbits were embedded in chaotic attractors. Thus, the observed periodic window replication, in the analyzed smooth continuous time dynamical systems, is an effective oscillator control process, once chaos is suppressed in determined parameter space regions.

Acknowledgements

This work was made possible by partial financial support from the following Brazilian government agencies: FAPESP, CNPq, and Capes.

References

[1] Gallas JAC. Structure of the parameter space of the Hénon map. Phys Rev Lett 1993;70:2714.
[2] Gallas JAC. Dissecting shrimps: results for some one-dimensional physical models. Physica A 1994;202:196.
[3] Lorenz EN. Compound windows of the Hénon-map. Physica D 2008;237:1689.

[4] Ullmann K, Caldas IL. Transitions in the parameter space of a periodically forced dissipative system. Chaos Solitons Fract 1996;7:1913.
[5] de Souza SLT, Wiercigroch M, Caldas IL, Balthazar JM. Suppressing grazing chaos in impacting system by structural nonlinearity. Chaos Solitons Fract 2008;38:864.
[6] Baptista MS, Caldas IL. Dynamics of the kicked logistic map. Chaos Solitons Fract 1996;7:325.
[7] Bonatto C, Garreau JC, Gallas JAC. Self-similarities in the frequency-amplitude space of a loss-modulated CO_2 laser. Phys Rev Lett 2005;95:143905.
[8] Freire JG, Gallas JAC. Non-shilnikov cascades of spikes and hubs in a semiconductor laser with optoelectronic feedback. Phys Rev E 2010;82:037202.
[9] Bonatto C, Gallas JAC. Accumulation boundaries: codimensional-two accumulation of accumulations in phase diagrams of semiconductor lasers, electric circuits, atmospheric and chemical oscillators. Phil Trans R Soc A 2008;366:505.
[10] Ramírez-Ávila GM, Gallas JAC. How similar is the performance of the cubic and piecewise-linear circuits of Chua? Phys Lett A 2010;375:143.
[11] Cardoso JCD, Albuquerque HA, Rubinger RM. Complex periodic structures in bi-dimensional bifurcations diagrams of a RLC circuit model with a nonlinear NDC device. Phys Lett A 2009; 373:2050.
[12] de Souza SLT, Caldas IL, Viana RL. Multistability and self-similarity in the parameter space of a vibro-impact system. Math Probl Eng 2009;2009:290356.
[13] Slipantschuk J, Ullner E, Baptista MS, Zeineddine M, Thiel M. Abundance of stable periodic behavior in a Red Grouse population model with delay: a consequence of homoclinicity. Chaos 2010;20:045117.
[14] Stoop R, Benner P, Uwate Y. Real-world existence and origins of the spiral organization of Shrimp-shaped domains. Phys Rev Lett 2010;105:074102.
[15] Maranhão DM, Baptista MS, Sartorelli JC, Caldas IL. Experimental observation of a complex periodic window. Phys Rev E 2008;77: 037202.
[16] Viana Jr. ER, Rubinger RM, Albuquerque HA, de Oliveira AG, Ribeiro GM. High-resolution parameter space of an experimental chaotic circuit. Chaos 2010;20:023110.
[17] Medeiros ES, de Souza SLT, Medrano-T RO, Caldas IL. Periodic window arising in the parameter space of an impact oscillator. Phys Lett A 2010;374:2628.
[18] Kapitaniak T, Brindley J, Czolczynski K. In: Chen G, editor. Controlling chaos and bifurcations in engineering systems. Boca Raton: CRC Press LLC; 1999. p. 71–86.
[19] Zambrano S, Seoane JM, Mariño IP, Sanjuán MAF, Euzzor S, Meucci R, et al. Phase control of excitable systems. New J Phys 2008;10:073030.
[20] Lima R, Pettini M. Suppression of chaos by resonant parametric perturbations. Phys Rev A 1990;41:726.
[21] Qu Z, Hu G, Yang G, Qin G. Phase effect in taming nonautonomous chaos by weak harmonic perturbations. Phys Rev Lett 1995;74:1736.
[22] Braiman Y, Goldhirsch I. Taming chaotic dynamics with weak periodic perturbations. Phys Rev Lett 1991;66:2545.
[23] Holmes P. A nonlinear oscillator with a strange attractor. Phil Trans R Soc A 1979;292:419.
[24] Chacón R. General results on chaos suppression for biharmonically driven dissipative systems. Phys Lett A 1999;257:293.
[25] Bonatto C, Gallas JAC, Ueda Y. Chaotic phase similarities and recurrences in a damped-driven Duffing oscillator. Phys Rev E 2008;77:262171.
[26] Moon FC. Fractal boundary for chaos in a two-state mechanical oscillator. Phys Rev Lett 1984;53:962.
[27] Wolf A, Swift JB, Swinney HL, Vastano JA. Determining Lyapunov exponents from a time series. Physica D 1985;16:285.
[28] Stewart WC. Current-voltage characteristics of Josephson junctions. Appl Phys Lett 1968;12:277.
[29] Cicogna G, Fronzoni L. Effects of parametric perturbations on the onset of chaos in the Josephson-junction model: theory and analog experiments. Phys Rev A 1990;42:1901.
[30] Cirillo M, Pedersen NF. On bifurcations and transitions to chaos in a Josephson junction. Phys Lett A 1982;90:150.
[31] Chacón R, Palmero F, Balibrea F. Taming chaos in a driven Josephson junction. Int J Bifurcat Chaos 2001;11:1897.